University of New Mexico

UNM Digital Repository

4-1-2022

Femur morphology in healthy infants and young children

Nathan P. Brown
Department of Bioengineering, J.B. Speed School of Engineering, University of Louisville, Louisville, Kentucky, USA

Angela Thompson
Department of Engineering Fundamentals, J.B. Speed School of Engineering, University of Louisville, Louisville, Kentucky, USA

Karen Bertocci
Department of Bioengineering, J.B. Speed School of Engineering, University of Louisville, Louisville, Kentucky, USA

Natalie L. Adolphi
Department of Biochemistry and Molecular Biology, University of New Mexico, Albuquerque, New Mexico, USA

Lauren Dvorscak
Department of Pathology, University of New Mexico, Albuquerque, New Mexico, USA

See next page for additional authors

Follow this and additional works at: https://digitalrepository.unm.edu/hsc_path_pubs

Recommended Citation

Bertocci G, Brown NP, Thompson A, Bertocci K, Adolphi NL, Dvorscak L, Pierce MC. Femur morphology in healthy infants and young children. Clin Anat. 2022 Apr;35(3):305-315. doi: 10.1002/ca.23825. Epub 2021 Dec 22. PMID: 34881441.

Authors

Nathan P. Brown, Angela Thompson, Karen Bertocci, Natalie L. Adolphi, Lauren Dvorscak, Mary Clyde
Pierce, and Gina Bertocci

ORIGINAL COMMUNICATION

Femur morphology in healthy infants and young children

Gina Bertocci[1] [ORCID] | Nathan P. Brown[1] | Angela Thompson[2] | Karen Bertocci[1] | Natalie L. Adolphi[3] | Lauren Dvorscak[4] | Mary Clyde Pierce[5]

[1]Department of Bioengineering, J.B. Speed School of Engineering, University of Louisville, Louisville, Kentucky, USA

[2]Department of Engineering Fundamentals, J.B. Speed School of Engineering, University of Louisville, Louisville, Kentucky, USA

[3]Department of Biochemistry and Molecular Biology, University of New Mexico, Albuquerque, New Mexico, USA

[4]Department of Pathology, University of New Mexico, Albuquerque, New Mexico, USA

[5]Division of Emergency Medicine, Ann & Robert H. Lurie Children's Hospital of Chicago, Chicago IL and Department of Pediatrics, Northwestern University Feinberg School of Medicine, Northwestern University, Chicago, Illinois, USA

Correspondence
Gina Bertocci, Department of Bioengineering, J.B. Speed School of Engineering, University of Louisville, 500 South Preston Street, Louisville, KY 40202, USA.
Email: g.bertocci@louisville.edu

Abstract

The objective of this study was to characterize femur morphology in healthy infants and young children. Anterior–posterior (AP) radiographs of the femur from children age 0–3 years with no history of bone disease were obtained from two children's hospitals and one medical examiner's office. Femur morphological measures (bone length, minimum diaphysis diameter, growth plate width, and femur radius of curvature) and sectional structural measures were determined. Measures were described and compared based on subject age and mass. Relationships between measures and age and mass were evaluated. The 169 AP femur radiographs were obtained from 99 children (59.6% males, median age = 12.0 months, IQR = 0–27.5 months, median body weight = 10.0 kg, IQR = 4.4–15.6 kg). Femur length ($r_s = 0.97$, $p < 0.001$; $r_s = 0.89$, $p < 0.001$), trochanter width ($r_s = 0.86$, $p < 0.001$; $r_s = 0.85$, $p < 0.001$), minimum diaphysis diameter ($r_s = 0.91$, $p < 0.001$; $r_s = 0.87$, $p < 0.001$), and growth plate width ($r_s = 0.91$, $p < 0.001$; $r_s = 0.84$, $p < 0.001$) increased with age and weight, respectively. Cross-sectional area ($r_s = 0.87$; $r_s = 0.86$; $p < 0.01$), polar moment of inertia ($r_s = 0.91$; $r_s = 0.87$; $p < 0.001$), moment of inertia ($r_s = 0.91$; $r_s = 0.87$; $p < 0.001$), polar modulus ($r_s = 0.91$; $r_s = 0.87$; $p < 0.001$) and medullary canal diameter ($r_s = 0.83$, $p < 0.001$; $r_s = 0.73$, $p < 0.001$) at the minimum diaphysis also increased with age and weight, respectively. Changes during rapid bone growth are important to understanding fracture risk in infants and young children as they transition to independent walking. Femur length, trochanter width, minimum diaphysis diameter and growth plate width increased with age and weight. Structural properties associated with fracture resistance also increased with age and weight.

KEYWORDS
bone development, bone morphology, bone properties, child, femur

1 | INTRODUCTION

Healthy bone development is dependent upon multiple factors, including diet, hormones, genetics, and mechanical loading (Biewener & Betram, 1993; Dimeglio, 2001; Ruff, 2003a; Swan et al., 2020). Physiological loading and associated stresses and strains applied to bone are critical in the development of bone structure and strength needed to resist fracture (Biewener & Betram, 1993; Ruff, 2003a). Poor bone health can result in increased fracture risk in children exposed to even routine physiological loading conditions encountered in daily activities (Fortin et al., 2020; Morgan et al., 2018). Compromised bone health due to connective tissue disorders, metabolic conditions, neuromuscular disorders and severe chronic diseases often lead to an increased likelihood of fracture (Fortin et al., 2020; Morgan et al., 2018). Bone quality and morphology (geometry and structure) play an important role in bone resistance

Gina Bertocci and Nathan P. Brown are co-first authors.

to fracture (Li et al., 2015; Ruff, 2003a). Although bone quality (i.e., density) has previously been described in young children (Crabtree et al., 2014), there has been little focus on bone morphology in this population. Not only can morphological measures provide insight into resistance to fracture, but they may differ in healthy vs. unhealthy bone, providing a potential means to objectively differentiate between them and aid in diagnosis of unhealthy bone. Currently, radiologists typically distinguish between healthy and unhealthy bone using subjective assessment of bone morphology and quality from radiographs (Mulugeta et al., 2011).

Femur morphology rapidly changes during the first years of life (Li et al., 2015) but has not been sufficiently described in the developing child. In one study, mid-diaphysis diameter and femur length, defined as the distance between the proximal and distal ossification centers, were reported for children age 0–3 years (Li et al., 2015). Some studies have reported femoral characteristics in older children ranging in age from 2 months to 21.5 years (Ruff, 2003a) and 3.8–15.6 years old (Craig et al., 2004). Schlegl et al. described femoral characteristics including femur length, femoral head diameter, and femoral mechanical axis-femoral shaft angle for seven children <3 years of age, but of those six had idiopathic scoliosis, and one had an unknown diagnosis (Schlegl et al., 2017). Femoral growth plate morphology and surface area were measured in children and adolescents (3.8–15.6 years of age) using magnetic resonance imaging (MRI) (Craig et al., 2004), and healthy femur morphology has been described in detail for adult cadavers using computed tomography (CT) (Cho et al., 2015; Schmutz et al., 2017). However, femur morphology of young children differs substantially from adults. At birth, only the diaphysis is ossified, while the distal and proximal epiphyses gradually ossify from birth to toddlerhood (Li et al., 2015). Children typically cruise (ambulate with support) between 6 and 14 months of age and ambulate independently by 18 months of age (Sugar et al., 1999). During these developmental milestones, the biomechanical function of the femur transitions to accommodate increased loading through rapid bone deposition and structural development that accompanies a growth spurt and increase in femoral strength in late infancy (Ruff, 2003a). As ambulatory children grow, changes in ambulation patterns likely also affect femur development (Cowgill et al., 2010).

Quantification of femur growth and development in children can provide a basis to distinguish normal versus abnormal bone development (Dimeglio, 2001). For instance, diaphysis length generally increases with age during development; however, low-body weight or premature birth may lead to decreased diaphysis length compared to children of a similar age (Li et al., 2015). Additional factors that may disrupt femur growth and development include, but are not limited to, presence of a disability or metabolic bone disease (Albert et al., 2014; Modlesky et al., 2009). Total, cortical, and medullary volume and width, as well as cross-sectional area (CSA), moment of inertia, section modulus and polar moment of inertia were significantly decreased in children with quadriplegic cerebral palsy who were unable to ambulate independently as compared to age-matched controls (Modlesky et al., 2009). Additionally, maximum bone flexural strength was less in children with osteogenesis imperfecta compared to healthy pediatric bone (Albert et al., 2014). However,

characterization of healthy pediatric femoral morphology is needed to establish normative reference data for pediatric bone.

Pediatric radiologists determine bone health based on clinical expertise but typically do not use quantitative measures to differentiate healthy femurs from unhealthy femurs. Although MRIs and CTs provide enhanced detail and 3D viewing capability, plain film radiographs are currently the standard of care given lower radiation exposure, lower cost, greater availability, and shorter time required for image acquisition, processing, and review. Limited femoral morphological characteristics of healthy infants and young children have been described in only a few studies involving a small number of subjects (Li et al., 2015; Maresh, 1955; Ruff, 2003a), but more extensive radiographic morphological measures have not been reported. The objective of this study was to quantify femur morphology from anterior–posterior (AP) radiographs in healthy infants and children from 0 to 3 years of age.

2 | METHODS

Study procedures were approved by the University of Louisville Institutional Review Board (IRB #15.0263).
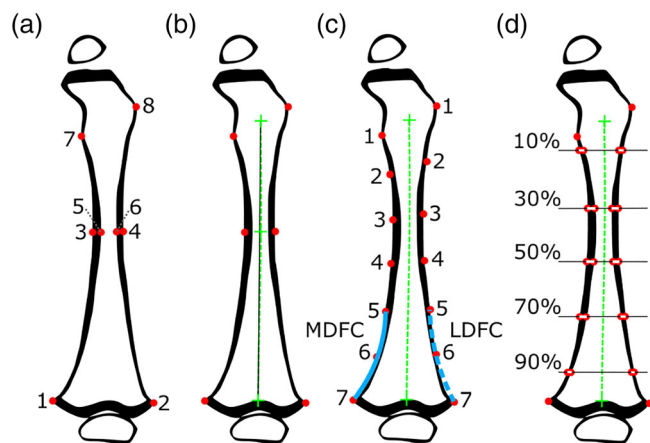
2.1 | Data collection

Medical records were retrospectively reviewed for children aged 0–3 years who had a femur radiograph from two children's hospitals and one medical examiner's office (Norton Children's Hospital, Louisville, KY; Children's Hospital of Pittsburgh, Pittsburgh, PA; New Mexico Office of the Medical Investigator, Albuquerque, NM). Children with a history of bone disease (e.g., osteogenesis imperfecta, rickets, osteopenia, and osteoporosis), conditions potentially affecting bone health (e.g., premature birth, spina bifida), or history of taking medications that could potentially influence bone health were excluded from the study. Questionable cases with no formal diagnosis of bone disease were reviewed by a study physician (Mary Clyde Pierce or Lauren Dvorscak) to determine whether the child's bone health may have been compromised by medications or other conditions; these cases were included/excluded from the study as appropriate. Deidentified AP femur radiographs from the left and/or right femur(s) were obtained, and radiology reports retrieved. Limbs with a fracture present were excluded from analysis. Age, height, weight, sex, race (Caucasian, Black, Asian/Pacific Islander, Native American Indian, one or more races, or unspecified/unknown), ethnicity (non-hispanic, hispanic, or unspecified/unknown), and mobility status (unknown, ambulatory, nonambulatory, cruises, or ambulatory with assistive device) were recorded when available. Body mass index was calculated from subject height and weight when available.

2.2 | Femur morphological assessment tool

A custom, user-guided image analysis tool was developed using mathematical analysis software (MATLAB R2016b, MathWorks,

—WILEY 307

Natick, MA) to perform key measurements from radiographs. The assessment tool guides the user to select points on the radiograph corresponding to bony landmark locations, which are then used to determine desired morphological measures. A radiograph scaling factor was used to scale measurements as appropriate. Points identified on the femur radiograph (Figure 1A) included the medial and lateral aspects of the distal femoral growth plate, the medial and lateral extent of the minimum diaphysis diameter (outer aspect of cortex), the medial and lateral extent of the medullary canal diameter (inner aspect of cortex) at the minimum diaphysis diameter, the lesser trochanter and greater trochanter. The assessment tool automatically determined the midpoint of the distal growth plate, midpoint of the minimum diaphysis diameter, and midpoint of the trochanter distance. The femur curvature was defined as the reciprocal of the radius of the arc passing through the distal growth plate midpoint, minimum diaphysis diameter midpoint, and trochanter midpoint (Figure 1B). The arc corresponding to the femur curvature was divided into thirds (proximal, mid, and distal), and the medial and lateral outer cortex curvatures were determined for the distal region using the arc determined from three equidistantly spaced points (Figure 1C). Medial and lateral inner and outer cortical walls were selected at 10%, 30%, 50%, 70%, and 90% along the femur (Figure 1D). One author (Nathan P. Brown) performed all radiograph assessments.

2.3 | Femur morphological measures

Using user-selected points on AP radiographs, key morphological measures were determined (Table 1). Normalized ratios of

TABLE 1 Femur morphological measures and definitions

Overall measures	
Distal growth plate width	Distance between the medial and lateral aspects of the distal femoral growth plate
Trochanter width	Distance between the lesser trochanter and greater trochanter
Femur length	Distance between the trochanter midpoint and distal growth plate midpoint
Curvature measures	
Femur curvature	Curvature (reciprocal of radius) of the arc passing through the midpoint of the distal growth plate width, midpoint of the minimum diaphysis diameter, and midpoint of the trochanter distance. Note: positive curvature is concave towards the body midline, negative is concave away from the body midline
Medial distal femoral curvature	Curvature (reciprocal of radius) of the arc passing through the medial distal fifth, sixth, and seventh points along the femur
Lateral distal femoral curvature	Curvature (reciprocal of radius) of the arc passing through the lateral distal fifth, sixth, and seventh points along the femur
Diaphyseal measures (determined at minimum diaphysis diameter and/or 10%, 30%, 50%, 70% and 90% of femur from the proximal end)	
Diaphysis diameter (outer diameter)	Distance between the medial and lateral outer cortex
Medial cortical wall thickness	Distance between the medial outer and inner cortex
Lateral cortical wall thickness	Distance between the lateral outer and inner cortex
Medullary canal diameter (inner diameter)	Distance between the medial and lateral extent of the inner cortex
Sectional measures (determined at minimum diaphysis diameter and 10%, 30%, 50%, 70% and 90% of femur from the proximal end)	
Cross-sectional area	$\frac{\pi}{4}\left(d_2^2 - d_1^2\right)$ — Area of an annulus where d_2 and d_1 are the diameter of the outer and inner aspects of the cortex, respectively
Moment of inertia	$\frac{\pi}{64}\left(d_2^4 - d_1^4\right)$ — Where d_2 and d_1 are the diameter of the outer and inner aspects of the cortex, respectively
Polar moment of inertia	$\frac{\pi}{32}\left(d_2^4 - d_1^4\right)$ — Where d_2 and d_1 are the diameter of the outer and inner aspects of the cortex, respectively
Polar modulus	$\frac{\pi}{32 d_2}\left(d_2^4 - d_1^4\right)$ — Where d_2 and d_1 are the diameter of the outer and inner aspects of the cortex, respectively

FIGURE 1 Bony landmark selection (red circles; the medial [1] and lateral [2] aspects of the distal femoral growth plate, the medial [3] and lateral [4] extent of the minimum diaphysis diameter [outer cortex], the medial [5] and lateral [6] extent of the medullary canal [inner aspect of cortex] at the minimum diaphysis diameter, the lesser trochanter [7] and greater trochanter [8]) (A), femur curvature (dashed green arc/line relative to solid straight black line) through the distal growth plate, minimum diaphysis width, and trochanter width midpoints (crosses) (B), medial distal femur curvature (MDFC, solid blue arc), and lateral distal femur curvature (LDFC, dashed blue arc) outer diaphysis curvatures determined using equidistance points 5–7 on the medial and lateral aspects, respectively (C), inner and outer diameters at 10%, 30%, 50%, 70%, and 90% along the femur (D). Representative femur is from a 12-month-old child

TABLE 2 Normalized femur morphological measures

Overall normalized measures
Minimum diaphysis diameter to distal growth plate width
Minimum diaphysis diameter to femur length
Femur length to distal growth plate width
Diaphyseal normalized measures (determined at minimum diaphysis diameter)
Medial cortical wall thickness to minimum diaphysis diameter
Lateral cortical wall thickness to minimum diaphysis diameter
Medial cortical wall thickness + lateral cortical wall thickness to minimum diaphysis diameter
Medial cortical wall thickness to femur length
Lateral cortical wall thickness to femur length
Medial cortical wall thickness + lateral cortical wall thickness to femur length

TABLE 3 Demographics, ambulatory status, and anthropometrics

Demographics and ambulatory status ($n = 99$)		Percent
Gender	Male	59.6%
	Female	40.4%
Race	Caucasian	64.6%
	Black	7.1%
	Asian/Pacific Islander	1.0%
	Native American	23.2%
	Unknown	4.0%
Ethnicity	Non-hispanic	54.5%
	Hispanic	24.2%
	Unknown	21.2%
Ambulatory status	Nonambulatory	36.4%
	Cruisers	4.0%
	Ambulatory	45.5%
	Unknown	14.1%

Anthropometrics	Median	Interquartile range
Age ($n = 99$)	12.0 months	0–27.5 months
Weight ($n = 99$)	10.0 kg	4.4–15.6 kg
Height ($n = 85$)	77.0 cm	58.0–95.0 cm
BMI ($n = 85$)	16.2 kg/m^2	13.3–19.1 kg/m^2

morphological measures were also determined (Table 2). All measures were recorded in a research database along with subject characteristics and radiographic images. Sectional measures in Table 1 were included to investigate structural characteristics that influence femur resistance to fracture.

2.4 | Data analysis

Intraclass correlation coefficient was used to determine intrarater reliability for landmark point selection when using the femur morphological assessment tool. A subset of measures was used to evaluate intrarater reliability; they included CSA determined along the femur, femur length, femur curvature, distal growth plate width, lateral cortical thickness determined along the femur, medial distal femur curvature, and diaphysis diameter determined along the femur. These measures were selected to capture different morphological aspects of the femur. These measures were evaluated twice on ten unique radiographs by the same author (Nathan P. Brown).

Femur morphological measures were characterized using descriptive statistics. Relationships between measures and age and body mass were determined using Spearman's rank order correlation coefficient as data were not normally distributed. All statistical analysis was performed using SPSS® Statistics Ver. 26 (IBM, 2020). All two-sided p-values were considered statistically significant at $p < 0.05$.

3 | RESULTS

AP radiographs of 169 femurs (left and right) were obtained for 99 children with demographics and anthropometrics as indicated in Table 3.

Radiographs from 14 children were from Norton Children's Hospital, Louisville, KY, 17 were from Children's Hospital of Pittsburgh, Pittsburgh, PA, and 68 were from New Mexico Office of the Medical
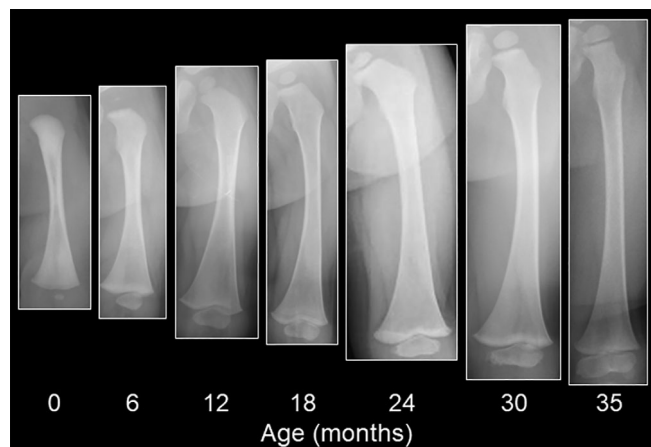
Investigator, Albuquerque, NM. Radiographs from representative children across our study age range illustrated overall femur development and morphological progression (Figure 2).

Femur length ($r_s = 0.97$, $p < 0.001$), trochanter width ($r_s = 0.86$, $p < 0.001$), minimum diaphysis diameter ($r_s = 0.91$, $p < 0.001$), growth plate width ($r_s = 0.91$, $p < 0.001$), and medullary canal diameter (inner diameter) at the minimum outer diaphysis diameter ($r_s = 0.83$, $p < 0.001$) were highly correlated with age (Figure 3). Trochanter width, minimum diaphysis diameter and growth plate width began plateauing at 12–18 months. Femur length ($r_s = 0.89$, $p < 0.001$), trochanter width ($r_s = 0.85$, $p < 0.001$), minimum diaphysis diameter ($r_s = 0.87$, $p < 0.001$), growth plate width ($r_s = 0.84$, $p < 0.001$), and medullary canal diameter at the minimum outer diaphysis diameter ($r_s = 0.73$, $p < 0.001$) were correlated with body weight (Figure 3). Femur curvature was primarily positive indicating concavity towards the midline of the body but trended towards 0 (i.e., straight femur) as age increased. Femur curvature did not correlate ($r_s \leq -0.52$) with age or weight.

CSA ($r_s = 0.87$ for age; $r_s = 0.86$ for weight; $p < 0.001$), polar moment of inertia ($r_s = 0.91$ for age; $r_s = 0.87$ for weight; $p < 0.001$), second moment of inertia ($r_s = 0.91$ for age; $r_s = 0.87$ for weight; $p < 0.001$), and polar modulus ($r_s = 0.91$ for age; $r_s = 0.87$ for weight; $p < 0.001$) evaluated at the minimum diaphysis diameter increased with age and body weight (Figure 4). Relationships between lateral cortical wall thickness and independent variables ($r_s = 0.65$ for age; $r_s = 0.62$ for weight; $p < 0.001$) were not as strong. Medial cortical wall thickness was correlated with weight ($r_s = 0.73$ for weight; $p < 0.001$).

Lateral distal femur curvature was relatively constant with age ($r_s = -0.26$, $p = 0.88$) and weight ($r_s = -0.01$, $p = 0.72$) (Figure 5). Medial distal femur curvature had a strong negative relationship with

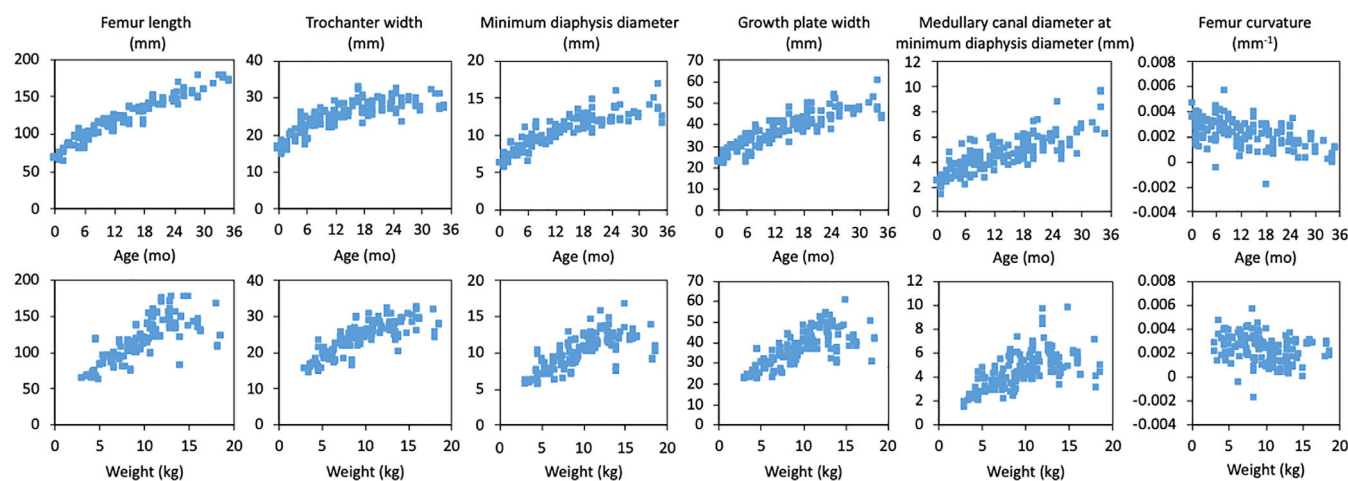age ($r_s = -0.85$; $p < 0.001$) trending towards straight, and a negative relationship with body weight ($r_s = -0.73$, $p < 0.001$) (Figure 5).

Key measures were normalized to minimum diaphysis diameter and femur length to determine whether they varied with age and weight. Lateral cortical wall thickness to diaphysis diameter, medial cortical wall thickness to diaphysis diameter, lateral cortical wall thickness to femur length, medial cortical wall thickness to femur length, lateral plus medial cortical wall thickness to diaphysis diameter, and lateral plus medial cortical wall thickness to femur length measured at the minimum diaphysis diameter were not correlated with age or weight ($r_s \leq 0.67$) (Figure 6).

Minimum diaphysis diameter to femur length (mean 0.09; SD ± 0.01) and minimum diaphysis diameter to growth plate width (mean 0.28; SD ± 0.02) were fairly constant across age ($r_s = -0.37$, $p < 0.001$; $r_s = 0.18$ $p < 0.001$, respectively) and weight ($r_s = -0.28$, $p < 0.001$; $r_s = 0.21$, $p < 0.001$, respectively) (Figure 7). Femur length to growth plate width (mean 3.14; SD ± 0.37) slightly increased with

FIGURE 2 Radiographs illustrating femur development across study age range of 0–35 months from representative healthy children. Radiographs are not to scale

FIGURE 3 Femur length, trochanter width, minimum diaphysis diameter, growth plate width, medullary canal diameter (inner diameter) at minimum diaphysis diameter, and femur curvature versus age and body weight for healthy children (n = 169 femurs)
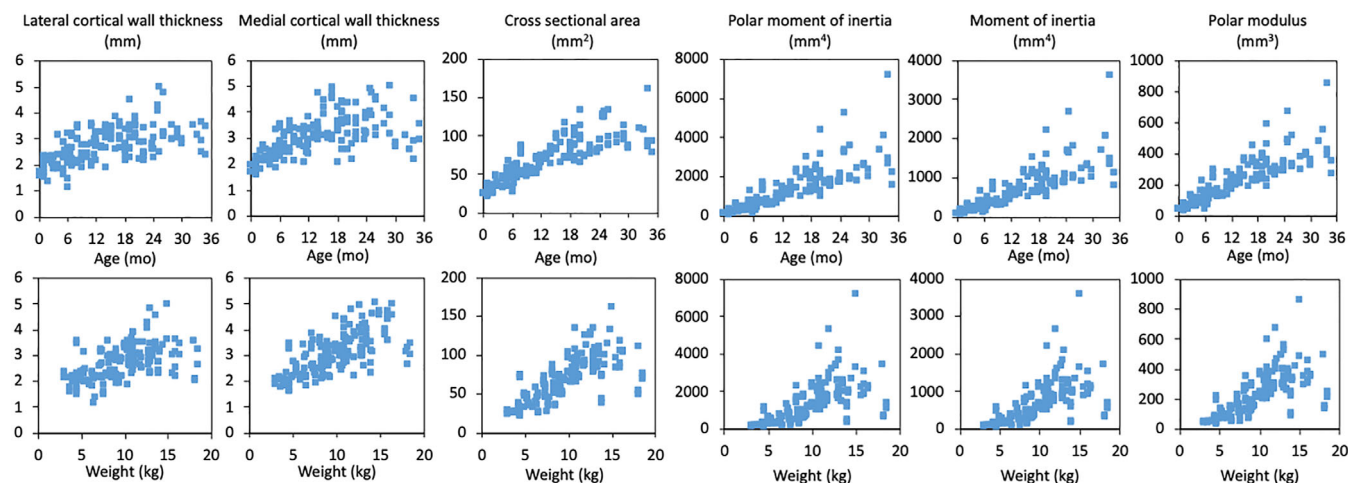
FIGURE 4 Lateral cortical wall thickness, medial cortical wall thickness, cross-sectional area (CSA), polar moment of inertia, moment of inertia, and polar modulus at the minimum diaphysis diameter versus age and body weight for healthy children (n = 169 femurs)

both age ($r_s = 0.47$, $p < 0.001$) and weight ($r_s = 0.41$, $p < 0.001$), but was not correlated with these measures (Figure 7).

Inner diameter, outer diameter, CSA, moment of inertia, polar moment of inertia, and polar modulus were determined along the length of the femur (10%, 30%, 50%, 70%, and 90% - Figure 1D) with respect to age (Figure 8). As expected, inner and outer diameters were greatest at the proximal (10%) and distal (70% and 90%) ends of the femur, and generally increased with age; the greatest increases with age were found at the distal femur (90%). CSA tended to increase with age, with greater CSAs at the proximal (10% and 30%) and central regions of the femur. Sectional measures were greatest at the distal end of the femur and generally increased with age at each location along the femur. Most notably, moment of inertia, polar moment of inertia and polar modulus were lowest at the central regions (30% and 50%) of the femur, coinciding with the cortex being closer to the neutral (longitudinal) axis of the bone.

In general, intrarater reliability was good for most measures but decreased for lateral cortical measures obtained at the proximal and distal femur, as well as for curvature of the femur (Table 4).

4 | DISCUSSION

In this study we have provided a detailed morphological description of the femur in children from 0–3 years of age using AP radiographs. During this period of rapid growth, overall morphology measures (femur length, trochanter width, and growth plate width) increased with age and weight. Diaphyseal measures and sectional measures obtained at the minimum diaphysis location (minimum diaphysis diameter, medullary canal diameter, lateral cortical wall thickness, medial cortical wall thickness, CSA, polar moment of inertia, moment of inertia, and polar modulus) also increased with both age and weight. Some measures (e.g., trochanter width, minimum diaphysis diameter, growth plate width and cortical thickness) tended to plateau starting at 12 to 18 months of age, which coincides with independent walking. These relationships between morphology measures and child age and weight describe trajectories of healthy bone development in infants and young children and can potentially aid in the differentiation of healthy vs. unhealthy bone. Measures characterizing bone structure (i.e., cortical CSA, moments of inertia and modulus) are of particular interest given their previously described direct correlation with resistance to fracture and their usefulness in characterizing the biomechanical effects of locomotion on the femur (Cowgill et al., 2010; Cowgill & Johnston, 2018; Ruff, 2003a). Their increase with age and weight suggests a decreasing fracture risk with the transition from
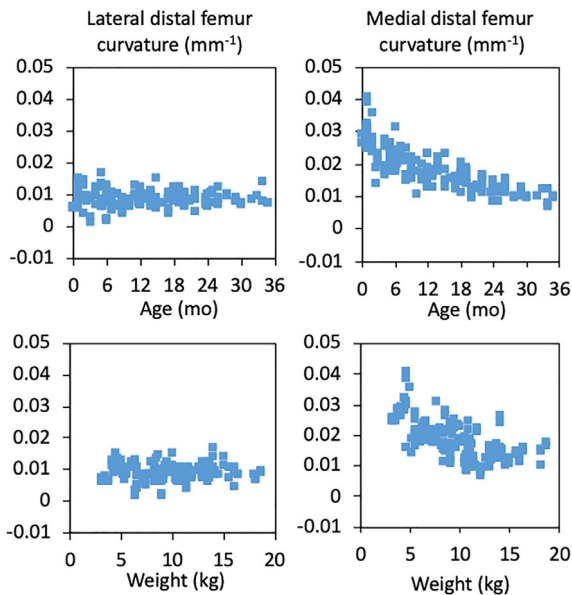

FIGURE 5 Medial and lateral distal femur outer diaphysis curvature plotted versus age and body weight for healthy children ($n = 169$)
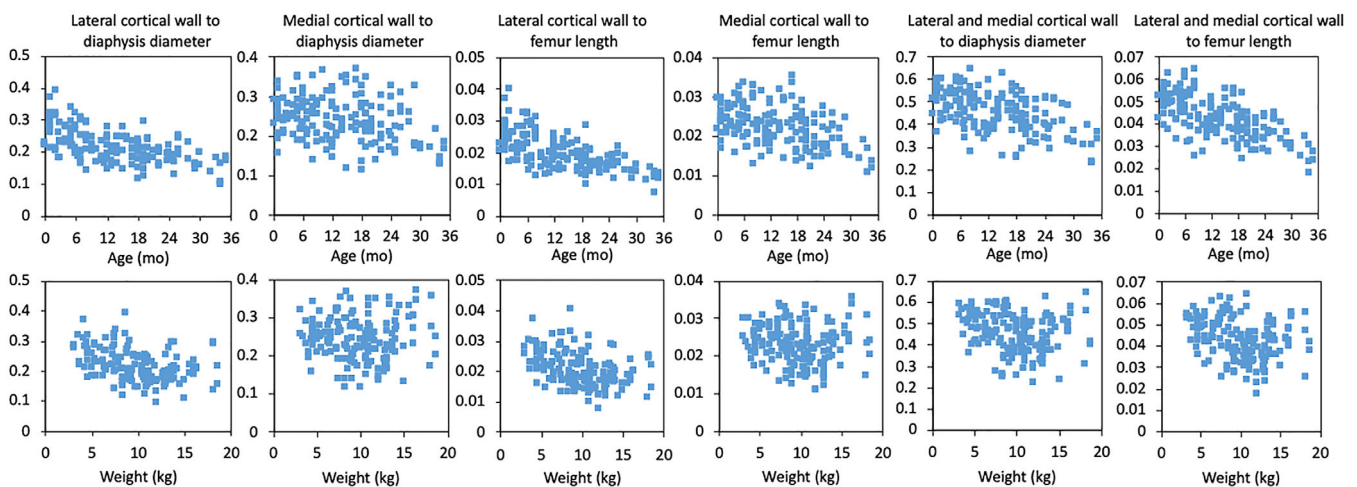
FIGURE 6 Lateral cortical wall thickness, medial cortical wall thickness, and lateral plus medial cortical wall thickness at the minimum diaphysis diameter normalized to minimum diaphysis diameter and femur length versus age and body weight for healthy children ($n = 169$ femurs)

FIGURE 7 Femur length to growth plate width, minimum diaphysis diameter to femur length, and minimum diaphysis diameter to growth plate width plotted versus age and weight for healthy children (*n* = 169 femurs)
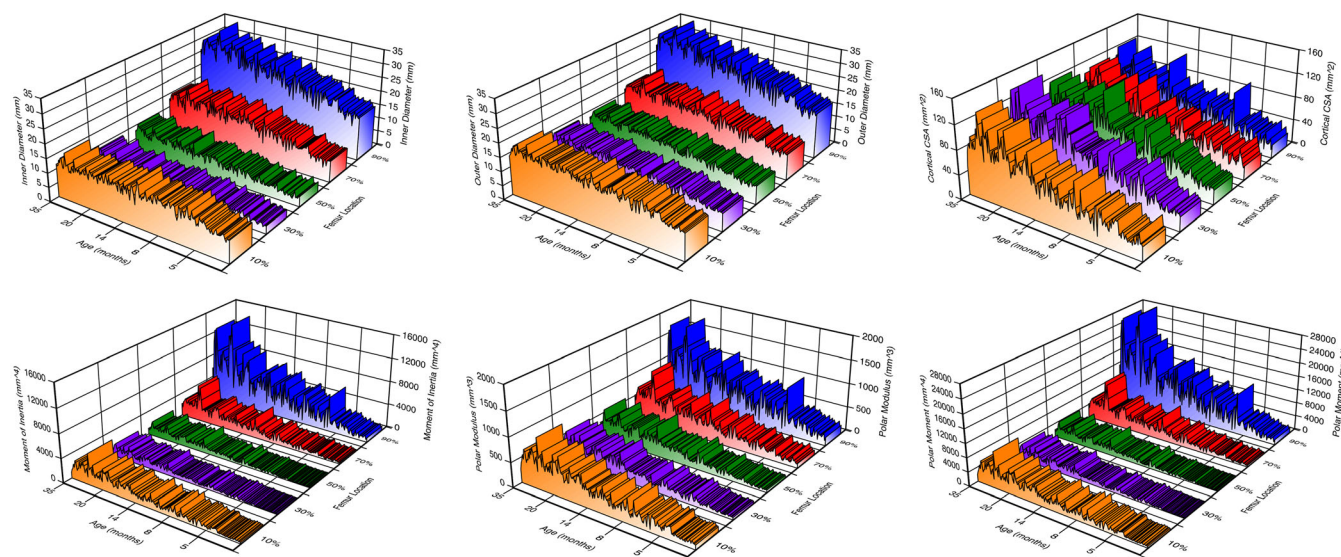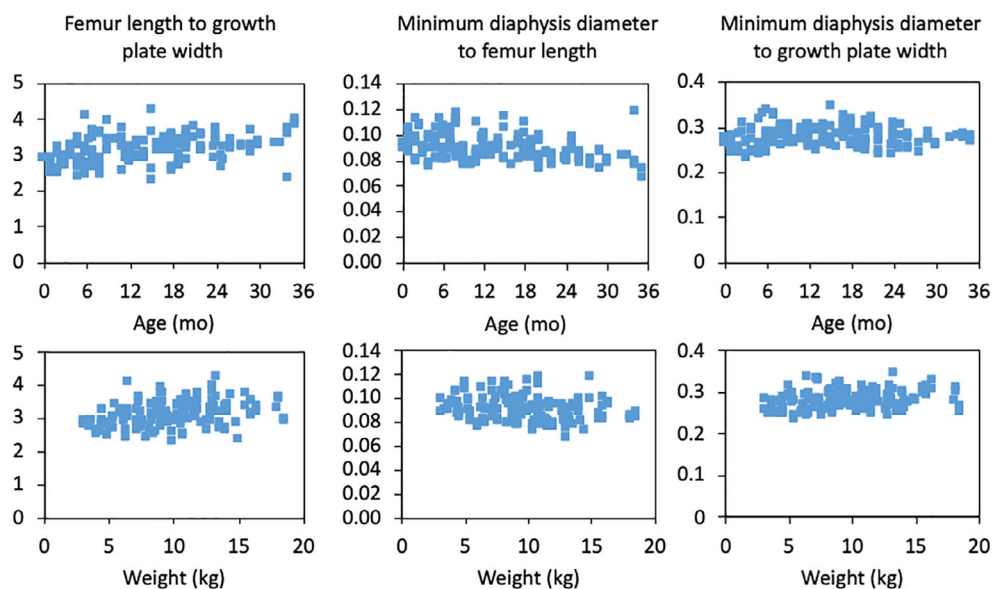
FIGURE 8 Inner diameter, outer diameter, cortical cross-sectional area (CSA), moment of inertia, polar modulus and polar moment of inertia at proximal (10%) to distal (90%) femur locations versus age for healthy children (*n* = 169 femurs)

infancy to toddlerhood as skeletal loading on the lower extremity increases with independent walking (Cowgill et al., 2010). A similar trend of rapidly increasing cortical CSA from 0 to 3 years of age was identified by Swan et al (Swan et al., 2020). We also found that a subset of normalized measures exhibited minimal variation across age and weight; femur length and minimum diaphysis diameter to growth plate width and minimum diaphysis diameter to femur length were nearly constant across age and weight. These normalized measures, which can be easily obtained in a clinical setting are a further step towards characterizing healthy bone in developing infants and children and may aid in delineating between healthy and unhealthy bone given their nearly constant ranges.

Femur length, diaphysis diameter, and growth plate width increased nearly linearly with age which is in agreement with others

who reported a strong positive correlation between femur length and age (Schlegl et al., 2017), an increase in diaphysis diameter with age (Li et al., 2015), and a linear increase in growth plate area (Craig et al., 2004) with age. Others have reported that the ratio of AP to medial-lateral moment of inertia linearly increased with age, but found a ratio < 1 in those younger than 4 years of age (Cowgill et al., 2010). Although the ratio of AP to medial-lateral moment of inertia was not evaluated in this study, the approximated annular CSA and sectional measures including moment of inertia did increase with age.

In our cohort of healthy children, we found that overall femur curvature exhibited concavity towards the midline of the body at younger ages but trended towards a straighter femur as age increased. Femur curvature was defined as the curvature (reciprocal of radius) of the arc passing through the midpoint of the distal growth plate width,

TABLE 4 Intraclass correlation coefficients and confidence intervals for femur measurements using the femur morphology assessment tool

Measurement	ICC[a]	95% CI lower upper	
Femur length	0.999	0.998	1
Femur curvature	0.743	0.283	0.928
Distal growth plate width	0.995	0.981	0.999
Lateral cortical thickness (proximal)	0.665	0.079	0.906
Lateral cortical thickness (mid-diaphysis)	0.867	0.556	0.965
Lateral cortical thickness (distal)	0.685	−0.007	0.919
Medial distal femur curvature	0.964	0.866	0.991
Diaphysis diameter (proximal)	0.992	0.961	0.998
Diaphysis diameter (mid-diaphysis)	0.998	0.992	0.999
Diaphysis diameter (distal)	0.997	0.985	0.999

[a]ICC (3, 1): Two-way mixed model, single measure, and absolute agreement.

midpoint of the minimum diaphysis diameter, and midpoint of the tro-chanter distance. Though we have not seen other reports of femur curvature in healthy children, bowing is common in disorders such as osteogenesis imperfecta and rickets, thus curvature may be an important factor in distinguishing healthy and unhealthy femurs. Bondioni et al. investigated angulation and bowing in unhealthy femurs by measuring the angle between the proximal and distal segments along the longitudinal axis (Bondioni et al., 2017). Increased angulation and bowing were found in fetal femurs with osteogenesis imperfecta type 2 and thanatophoric dysplasia bone diseases (Bondioni et al., 2017), while straighter femurs were found in those without bone disorders. Our findings of femoral straightening with increasing age corresponds with functional biomechanical changes (e.g., increased femoral strength) associated with weight bearing and independent ambulation occurring near 12 months of age (Martorell et al., 2006; Ruff, 2003a).

Though this is the first study to provide a comprehensive assessment of femur morphology in young children, our findings align with gross femur measurements (length, mid-shaft diameter) reported previously. Li et al. reported femoral lengths and diameters for 15 subjects aged 0–3 years (Li et al., 2015). Measurements were obtained from 3D models generated from CT scans. Femoral lengths, measured as the distance between proximal and distal ossification centers, increased with age from 7.7 cm in a 2-week-old child to 22.4 cm in a 3-year-old child. In our study, femur lengths were 15%–20% lower (6.2–18.8 cm over the same age range). However, this difference in femur length is expected given differing means of defining femoral length. We did not measure from the ossification centers to obtain femoral length as the epiphyses were not visible in younger infants. Li et al. also reported AP diameters at the mid-shaft ranging from approximately 5–17 mm in the youngest to oldest subjects (0–3 years). Our findings were comparable; minimum diaphysis diameter ranged from 5.6 to 16.8 mm.

We approximated the transverse diaphysis as a annular (circular) cross section, which is a reasonable approximation of the mid diaphysis in infants and young children (Cowgill et al., 2010); (Swan et al., 2020). The circular shape changes into a more ovate shape as the femur matures through adolescence, possibly due to transition
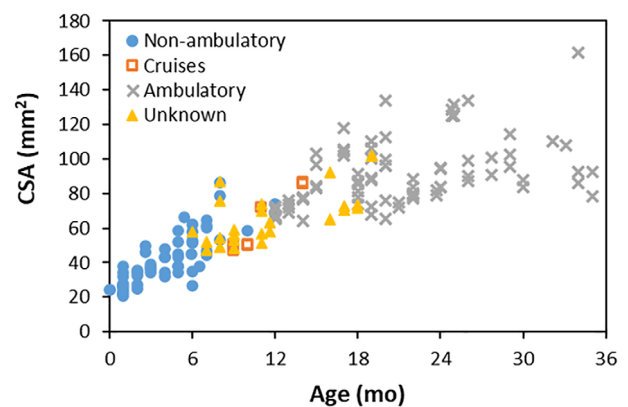
FIGURE 9 Cross-sectional area (CSA) at the minimum diaphysis diameter versus age based on mobility status

from biomechanical loading demands from a waddling, multidirectional gait in early ambulation to more unidirectional gait in older children, adolescents, and adults (Cowgill et al., 2010). Using micro-CT imaging, Swan et al. (Swan et al., 2020) found that femur cortical CSA increased with age and advancing mobility status in infants and children. Similarly, cortical CSA increased with age and advancing mobility status in our study (Figure 9). Children generally progressed from nonambulatory (0–6 months of age) to cruising (6–12 months of age) and finally ambulation (≥12 months of age), while at each advancing stage exhibiting increasing femoral CSA at the mid-diaphysis. CSA increased by 149% from the 0 to 6-month age range compared to >12-month age range and by 54% from the >6–12-month age range compared to the >12-month age range. Such increases in cortical CSA are evidence of bone structure adaptations to developmental stages in healthy infants and children as femoral loading patterns change with mobility status (Cowgill et al., 2010; Sumner & Andriacchi, 1996).

Swan et al. also found a decreasing cortical CSA to medullary canal area (MA) ratio with increasing age, with a notable change from a steep rate of decline to a plateau just before 1 year of age (at 50% of femur length), corresponding with weight bearing associated with
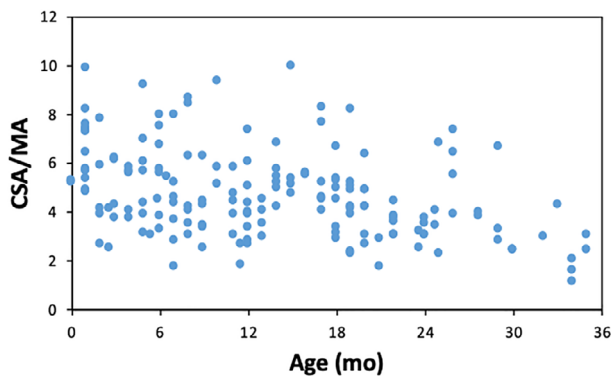
FIGURE 10 Cortical cross-sectional area (CSA) to medullary canal area (MA) at minimum diaphysis diameter versus age

cruising and ambulation. While our CSA/MA ratio fell within a similar range to that found by Swan et al., our data did not demonstrate a biphasic shape, but instead showed a gradual declining trend with increasing age (Figure 10). Although weight bearing dictates a need for robust bone structure (i.e., increased cortical CSA; Figure 9), it is important to note that bone remodeling is occurring and mineralization is increasing during this same period providing greater bone strength and improved resistance to fracture (Zimmermann et al., 2019). Zimmerman et al. found improvements in bone quality with bone growth between the ages of 1 and 2 years as evidenced by collagen fibril alignment and elevated mineralization to reinforce the collagen scaffold. These and other improvements in bone quality led to femoral mid-diaphyseal strength increases of 83% in children ≥2 years of age compared to fetal/infantile bone. From infancy through toddlerhood, both increases in CSA (documented in this study) and improvements in bone quality and strength (documented by others [Zimmermann et al., 2019]) would likely increase femoral resistance to fracture.

When using structural beam theory where the femur is approximated as a beam, CSA and related sectional measures describing bone structure are key to predicting bone resistance to fracture, with sectional measures representing resistance to fracture under differing loading conditions. For example, when a bone is loaded either axially or in shear, resistance to fracture is directly related to the cortex CSA; in other words, for given material properties, as CSA increases, bone can better withstand shear loading before yielding or fracturing. Similarly, when bone is exposed to a bending load, fracture resistance is directly related to femoral moment of inertia and the polar modulus, and when bone is under torsional loading, resistance to fracture is directly related to the polar moment of inertia. Since the predominant femoral loading condition during gait is bending, femoral moment of inertia and polar modulus can be thought of as bending rigidity representing biomechanical adaptation during bone development as children begin to cruise and independently walk (Rubin & Lanyon, 1982; Ruff, 2003b). In a longitudinal study of young children, Ruff (2003b) reported a mean polar modulus at the mid-diaphysis of 287 mm^3 (SD 1.18) for children 6 months old to 3 years of age (Ruff, 2003a). Similarly, our mean femoral polar modulus at the minimum diaphysis

diameter was 251 mm^3 (SD 151) for children 0–3 years of age. (Differences across studies may be due to the limited sample size [$n = 20$] and 6-month measurement intervals used by Ruff.) In both our study and Ruff (2003a), polar modulus increased linearly with age indicating greater resistance to bending stresses associated with the transition to independent walking. Interestingly, despite CSA being larger near the mid-diaphysis, structural properties such as moment of inertia and polar modulus tended to be higher at the distal femur and proximal femur, and lower near the mid-diaphysis (Figure 8). Even though cortical walls are substantially thicker at the mid-diaphysis, sectional structural properties are also dependent on spatial distribution of the bone relative to the longitudinal axis of the femur, thus leading to higher sectional measures at the distal femur. Thus, cortical bone tissue located further from the longitudinal center of the femur (i.e., at the proximal and distal regions of the femur) tends to increase these measures. However, the lower sectional measures at the mid-diaphysis are in part responsible for common fractures occurring in this region when the femur is subjected to bending loads that exceed fracture thresholds (Bertocci et al., 2017; Fortin et al., 2020).

Normative data for the femur in healthy children age 0–3 years of age established in this study could provide clinicians with characteristic morphology to evaluate and monitor bone growth. Additionally, this normative data can provide a basis for assessing bone health in infants and young children. Substantial deviation of femoral morphology from that presented here could indicate potential bone disease or development abnormality necessitating further clinical assessment. For instance, thin cortices or excessive curvature (i.e., bowing) may be indicative of osteogenesis imperfecta (OI) (Calder, 2015). Rickets-specific morphological characteristics may be more apparent in the distal femur through measures such as growth plate width or distal curvature (Calder, 2015). These features could differentiate healthy from unhealthy bone.

4.1 | Limitations

The goal of this study was to quantify femur morphology in infants and young children age 0–3 years. Bone is rapidly developing during this age range leading to substantial changes in bone morphology. Our study included 78 femurs in the 0–12 month age range, 56 in the 13–24 month age range, and 26 in the 25–36 month age range. Although to our knowledge this is the largest cohort of femurs used to evaluate detailed morphology in young children, differences in bone morphology across each age range may have influenced identification of bony landmarks given differences in ossification. However, intrarater reliability was generally strong across measures when assessing femurs from children of various ages. This study analyzed healthy bone. Selection of boney landmarks to characterize morphology may become more subjective using radiographs when analyzing unhealthy bone. For instance, the cortical walls may be less distinct due to decreased bone density or the presence of callus in healing bone which could distort measurements. In this study femur morphology was assessed using 2D AP radiographs. Bone morphology was not

determined using other radiographic views (e.g., medial-lateral) or through other imaging modalities such as 3D CT, which could aid in visualizing boney landmarks. Despite limitations of 2D radiographs, our findings were similar to those of Swan et al. and Li et al. who used CT imaging to assess femur morphology in infants and young children (Li et al., 2015; Swan et al., 2020). However, CT imaging is less suitable for widespread use in standard care given higher levels of radiation. Radiographs were obtained retrospectively in our study, and thus, radiography settings, and lower extremity placement and orientation were not controlled. Variation in lower extremity orientation could have influenced morphological measures, especially curvature measures. Differences in image quality and resolution across radiographs or radiographic distortion could have affected point selection using the femur morphological assessment tool. Finally, we did not delineate femur morphology based on sex.

5 | CONCLUSION

Comprehensive normative pediatric femur morphology data is important to characterizing typical bone development in healthy children. In children 0–3 years of age, femur length, trochanter width, minimum diaphysis diameter, medullary canal diameter and growth plate width increased with age and weight. Femur curvature tended to straighten with increasing age. Sectional structural measures including CSA, moment of inertia, polar moment of inertia and polar modulus evaluated at the minimum diaphysis also increased with age and weight. These changes during a period of rapid bone growth are important to understanding fracture risk in infants and young children as they transition to independent walking. Pediatric femur morphology data obtained from healthy children in this study can be used to objectively assess bone health by differentiating normal from abnormal development or healthy from diseased bone.

ORCID

Gina Bertocci 🄳 https://orcid.org/0000-0002-3697-3950

REFERENCES

Albert, C., Jameson, J., Smith, P., & Harris, G. (2014). Reduced diaphyseal strength associated with high intracortical vascular porosity within long bones of children with osteogenesis imperfecta. *Bone*, *66*, 121–130. https://doi.org/10.1016/j.bone.2014.05.022

Bertocci, G., Thompson, A., & Pierce, M. C. (2017). Femur fracture biomechanics and morphology associated with torsional and bending loading conditions in an in vitro immature porcine model. *Journal of Forensic and Legal Medicine*, *52*, 5–11. https://doi.org/10.1016/j.jflm.2017.07.021

Biewener, A., & Betram, J. (1993). Mechanical loading and bone growth in vivo. In B. Hall (Ed.), *Bone* (Vol. 7, 1st ed.). CRC Press.

Bondioni, M. P., Pazzaglia, U. E., Izzi, C., Di Gaetano, G., Laffranchi, F., Baldi, M., & Prefumo, F. (2017). Comparative X-ray morphometry of prenatal osteogenesis imperfecta type 2 and thanatophoric dysplasia: A contribution to prenatal differential diagnosis. *La Radiologia Medica*, *122*(11), 880–891. https://doi.org/10.1007/s11547-017-0784-0

Calder, A. D. (2015). Radiology of Osteogenesis Imperfecta, rickets and other bony fragility states. *Endocrine Development*, *28*, 56–71. https://doi.org/10.1159/000380992

Cho, H. J., Kwak, D. S., & Kim, I. B. (2015). Morphometric evaluation of Korean femurs by geometric computation: Comparisons of the sex and the population. *BioMed Research International*, *2015*, 730538. https://doi.org/10.1155/2015/730538

Cowgill, L. W., & Johnston, R. A. (2018). Biomechanical implications of the onset of walking. *Journal of Human Evolution*, *122*, 133–145. https://doi.org/10.1016/j.jhevol.2018.06.003

Cowgill, L. W., Warrener, A., Pontzer, H., & Ocobock, C. (2010). Waddling and toddling: The biomechanical effects of an immature gait. *American Journal of Physical Anthropology*, *143*(1), 52–61. https://doi.org/10.1002/ajpa.21289

Crabtree, N. J., Arabi, A., Bachrach, L. K., Fewtrell, M., El-Hajj Fuleihan, G., Kecskemethy, H. H., Jaworski, M., Gordon, C. M., & International Society for Clinical, D. (2014). Dual-energy X-ray absorptiometry interpretation and reporting in children and adolescents: The revised 2013 ISCD pediatric official positions. *Journal of Clinical Densitometry*, *17*(2), 225–242. https://doi.org/10.1016/j.jocd.2014.01.003

Craig, J. G., Cody, D. D., & Van Holsbeeck, M. (2004). The distal femoral and proximal tibial growth plates: MR imaging, three-dimensional modeling and estimation of area and volume. *Skeletal Radiology*, *33*(6), 337–344. https://doi.org/10.1007/s00256-003-0734-x

Dimeglio, A. (2001). Growth in pediatric orthopaedics. *Journal of Pediatric Orthopedics*, *21*(4), 549–555.

Fortin, K., Bertocci, G., Nicholas, J. L., Lorenz, D. J., & Pierce, M. C. (2020). Long bone fracture characteristics in children with medical conditions linked to bone health. *Child Abuse & Neglect*, *103*, 104396. https://doi.org/10.1016/j.chiabu.2020.104396

Li, X., Viceconti, M., Cohen, M. C., Reilly, G. C., Carre, M. J., & Offiah, A. C. (2015). Developing CT based computational models of pediatric femurs. *Journal of Biomechanics*, *48*(10), 2034–2040. https://doi.org/10.1016/j.jbiomech.2015.03.027

Maresh, M. M. (1955). Linear growth of long bones of extremities from infancy through adolescence; continuing studies. *American Journal of Diseases of Children*, *89*(6), 725–742.

Martorell, R., de Onis, M., Martines, J. C., Black, M., Onyango, A. W., & Dewey, K. G. (2006). WHO motor development study: Windows of acheivement for six gross motor development milestones. *Acta Paediatrica*, *95*, 86–95.

Modlesky, C. M., Kanoff, S. A., Johnson, D. L., Subramanian, P., & Miller, F. (2009). Evaluation of the femoral midshaft in children with cerebral palsy using magnetic resonance imaging. *Osteoporosis International*, *20*(4), 609–615. https://doi.org/10.1007/s00198-008-0718-8

Morgan, E. F., Unnikrisnan, G. U., & Hussein, A. I. (2018). Bone mechanical properties in healthy and diseased states. *Annual Review of Biomedical Engineering*, *20*, 119–143. https://doi.org/10.1146/annurev-bioeng-062117-121139

Mulugeta, P. G., Jordanov, M., Hernanz-Schulman, M., Yu, C., & Kan, J. H. (2011). Determination of osteopenia in children on digital radiography compared with a DEXA reference standard. *Academic Radiology*, *18*(6), 722–725. https://doi.org/10.1016/j.acra.2011.01.009

Rubin, C. T., & Lanyon, L. E. (1982). Limb mechanics as a function of speed and gait: A study of functional strains in the radius and tibia of horse and dog. *The Journal of Experimental Biology*, *101*, 187–211.

Ruff, C. (2003a). Growth in bone strength, body size, and muscle size in a juvenile longitudinal sample. *Bone, 33*(3), 317–329.

Ruff, C. (2003b). Ontogenetic adaptation to bipedalism: Age changes in femoral to humeral length and strength proportions in humans, with a comparison to baboons. *Journal of Human Evolution, 45*(4), 317–349. https://doi.org/10.1016/j.jhevol.2003.08.006

Schlegl, A. T., O'Sullivan, I., Varga, P., Than, P., & Vermes, C. (2017). Determination and correlation of lower limb anatomical parameters and bone age during skeletal growth (based on 1005 cases). *Journal of Orthopaedic Research, 35*(7), 1431–1441. https://doi.org/10.1002/jor.23390

Schmutz, B., Kmiec, S., Jr., Wullschleger, M. E., Altmann, M., & Schuetz, M. (2017). 3D computer graphical anatomy study of the femur: A basis for a new nail design. *Archives of Orthopaedic and Trauma Surgery, 137*(3), 321–331. https://doi.org/10.1007/s00402-016-2621-7

Sugar, N. F., Taylor, J. A., & Feldman, K. W. (1999). Bruises in infants and toddlers: Those who don't cruise rarely bruise. Puget Sound pediatric research network. *Archives of Pediatrics & Adolescent Medicine, 153*(4), 399–403.

Sumner, D. R., & Andriacchi, T. P. (1996). Adaptation to differential loading: Comparison of growth-related changes in cross-sectional properties of the human femur and humerus. *Bone, 19*(2), 121–126. https://doi.org/10.1016/8756-3282(96)00166-4

Swan, K. R., Ives, R., Wilson, L. A. B., & Humphrey, L. T. (2020). Ontogenetic changes in femoral cross-sectional geometry during childhood locomotor development. *American Journal of Physical Anthropology, 173*(1), 80–95. https://doi.org/10.1002/ajpa.24080

Zimmermann, E. A., Riedel, C., Schmidt, F. N., Stockhausen, K. E., Chushkin, Y., Schaible, E., Gludovatz, B., Vettorazzi, E., Zontone, F., Puschel, K., Amling, M., Ritchie, R. O., & Busse, B. (2019). Mechanical competence and bone quality development during skeletal growth. *Journal of Bone and Mineral Research, 34*(8), 1461–1472. https://doi.org/10.1002/jbmr.3730